Title

Static pushover analyses of pile groups in liquefied and laterally spreading ground in centrifuge tests

Journal

Journal of Geotechnical and Geoenvironmental Engineering, 133(9)

ISSN

1090-0241

Authors

Brandenberg, Scott J
Boulanger, R W
Kutter, Bruce L
et al.

Publication Date

2007-09-01

Peer reviewed

Static Pushover Analyses of Pile Groups in Liquefied and Laterally Spreading Ground in Centrifuge Tests

Scott J. Brandenberg, A.M.ASCE[1]; Ross W. Boulanger, M.ASCE[2]; Bruce L. Kutter, M.ASCE[3]; and Dongdong Chang, S.M.ASCE[4]

Abstract: Monotonic, static beam on nonlinear Winkler foundation (BNWF) methods are used to analyze a suite of dynamic centrifuge model tests involving pile group foundations embedded in a mildly sloping soil profile that develops liquefaction-induced lateral spreading during earthquake shaking. A single set of recommended design guidelines was used for a baseline set of analyses. When lateral spreading demands were modeled by imposing free-field soil displacements to the free ends of the soil springs (BNWF_SD), bending moments were predicted within −8% to +69 (16th to 84th percentile values) and pile cap displacements were predicted within −6 to +38%, with the accuracy being similar for small, medium, and large motions. When lateral spreading demands were modeled by imposing limit pressures directly to the pile nodes (BNWF_LP), bending moments and cap displacements were greatly overpredicted for small and medium motions where the lateral spreading displacements were not large enough to mobilize limit pressures, and pile cap displacements were greatly underpredicted for large motions. The effects of various parameter relations and alternative design guidelines on the accuracy of the BNWF analyses were evaluated. Sources of bias and dispersion in the BNWF predictions and the issues of greatest importance to foundation performance are discussed. The results of these comparisons indicate that certain guidelines and assumptions that are common in engineering design can produce significantly conservative or unconservative BNWF predictions, whereas the guidelines recommended herein can produce reasonably accurate predictions.

DOI: 10.1061/(ASCE)1090-0241(2007)133:9(1055)

CE Database subject headings: Pile foundations; Pile caps; Earthquakes; Liquefaction; Centrifuge; Pile lateral loads; Soil deformation.

Introduction

Extensive damage to pile foundations has been caused by liquefaction and lateral spreading of the surrounding soils, and has been particularly intense when a nonliquefied crust spreads laterally on top of underlying liquefiable layers (e.g., JGS 1996, 1998). Mechanisms of interaction between piles and liquefied, spreading soils have become better understood in recent years through evaluation of case histories, centrifuge model studies, 1g model tests, full-scale field tests, and analytical studies (e.g., Boulanger and Tokimatsu 2006). These physical observations and research findings also provide the basis for evaluating the accuracy and limitations of analytical models and design guidelines.

Monotonic beam on nonlinear Winkler foundation (BNWF) analyses of pile group foundations in liquefied soil (Fig. 1) are evaluated using the suite of dynamic centrifuge model tests described by Brandenberg et al. (2005). The piles were modeled as beam–column elements, and soil–structure interaction was modeled using $p-y$ materials for lateral subgrade reaction, $t-z$ materials for pile shaft friction, and $q-z$ materials for pile tip end bearing. Demands from laterally spreading layers were represented by imposing free-field soil displacements (SD) on the free ends of the $p-y$ materials (BNWF_SD), and also by imposing limit pressures (LP) directly to the pile nodes (BNWF_LP). The BNWF_SD approach is more general than the BNWF_LP approach because the latter inherently assumes that soil displacements are large enough to mobilize the ultimate loads from the spreading crust and liquefiable layer against the pile group. The only benefit of using limit pressures instead of soil displacements is that force boundary conditions are sometimes easier to implement than displacement boundary conditions. Inertia forces were represented as static forces applied simultaneously with lateral spreading demands.

The paper proceeds by first presenting centrifuge test observations that directly address deficiencies and limitations in current guidelines for static BNWF analyses, followed by the description of proposed guidelines that address some of these deficiencies. A detailed comparison of predicted and measured bending moment and pile displacement distributions is presented for one example centrifuge event, after which predicted and measured peak bending moments and peak pile cap displacements are compared for

[1]Assistant Professor, Dept. of Civil and Environmental Engineering, Univ. of California at Los Angeles, Los Angeles, CA 90095. E-mail: sjbrandenberg@ucla.edu

[2]Professor, Dept. of Civil and Environmental Engineering, Univ. of California at Davis, Davis, CA 95616.

[3]Professor, Dept. of Civil and Environmental Engineering, Univ. of California at Davis, Davis, CA 95616.

[4]Senior Staff Engineer, Geosyntec Consultants, Inc., 475 14th St., Ste. 450, Oakland, CA 94612; formerly, Graduate Student, Dept. of Civil and Environmental Engineering, Univ. of California at Davis, Davis, CA 95616.

Note. Discussion open until February 1, 2008. Separate discussions must be submitted for individual papers. To extend the closing date by one month, a written request must be filed with the ASCE Managing Editor. The manuscript for this paper was submitted for review and possible publication on March 3, 2006; approved on July 14, 2006. This paper is part of the ***Journal of Geotechnical and Geoenvironmental Engineering***, Vol. 133, No. 9, September 1, 2007. ©ASCE, ISSN 1090-0241/2007/9-1055–1066/$25.00.

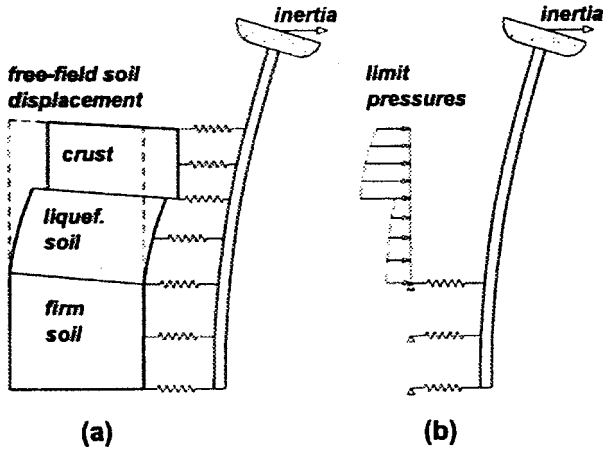

Fig. 1. BNWF analysis approach with (a) imposed free-field soil displacements (BNWF_SD); (b) imposed limit pressures (BNWF_LP)

the suite of centrifuge tests for one baseline set of parameters. Alternative design guidelines and approximations that might be considered reasonable based on current standard-of-practice approaches are subsequently evaluated against the centrifuge test data. Limitations inherent to static BNWF approaches and their implications for design are discussed. Finally, some aspects of BNWF design guidelines that particularly warrant further study are identified.

Centrifuge Tests

A series of dynamic tests was performed on the 9-m radius centrifuge at the University of California at Davis, Davis, Calif.

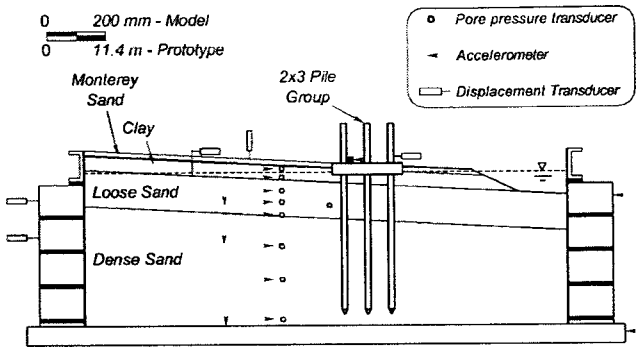

Fig. 2. Centrifuge model layout with most of the 100 instruments omitted for clarity

(Table 1). Details of the tests were presented by Brandenberg et al. (2005) and only an abbreviated summary is given herein. Fig. 2 shows the model layout for Centrifuge Test SJB03, which was similar to the four other tests analyzed herein. The soil profile for all of the models consisted of a nonliquefiable clay crust overlying loose sand (relative density, $D_r \approx 31-35\%$) overlying dense sand ($D_r \approx 75-83\%$). All of the layers sloped gently toward a river channel carved in the crust at one end of the model. The sand layers beneath the crust were uniformly-graded Nevada sand (uniformity coefficient, $C_u=1.5$; median grain size, $D_{50}=0.15$ mm). The nonliquefiable crust was composed of reconstituted San Francisco Bay mud (liquid limit ≈88, plasticity index ≈48) that was mechanically consolidated with a large hydraulic press, and subsequently carved to the desired slope. The undrained shear strength (s_u) averaged over the depth of the crust ranged from 22 to 44 kPa among the tests. A thin layer of coarse Monterey sand was placed on the surface of the Bay mud for some of the models. The model was saturated with water, as

Table 1. Soil and Pile Properties for Five Centrifuge Models

Test ID	Properties of six-pile group	Soil profile	N
PDS03	$b=0.73$ m, $I=4.5\times10^{-3}$ m^4 L, W, $H=9.5$, 5.7, 2.3 m $m_{cap}=374$ Mg	4.2 m clay ($s_u=22$ kPa,[a] $\gamma=15.5$ kN/m^3) Over 4.6 m loose sand ($D_r=31\%$, $\gamma=19$ kN/m^3) Over dense sand ($D_r=79\%$, $\gamma=20$ kN/m^3)	38.1g
SJB01	$b=0.73$ m, $I=4.5\times10^{-3}$ m^4 L, W, $H=10.1$, 6.5, 2.5 m $m_{cap}=374$ Mg	4.2 m clay ($s_u=44$ kPa)[a] Over 4.6 m loose sand ($D_r=33\%$) Over dense sand ($D_r=83\%$)	38.1g
SJB03	$b=1.17$ m, $I=24.0\times10^{-3}$ m^4 L, W, $H=14.3$, 9.2, 2.2 m $m_{cap}=726$ Mg	1.4 m coarse sand ($\gamma\approx17$ kN/m^3) Over 2.7 m clay ($s_u=44$ kPa,[a] $\gamma=16$ kN/m^3) Over 5.4 m loose sand ($D_r=35\%$) Over dense sand ($D_r=75\%$)	57.2g
DDC01	$b=1.17$ m, $I=24.0\times10^{-3}$ m^4 L, W, $H=14.3$, 9.2, 2.2 m Superstructure $T=0.8$ s[b] $m_{cap}=714$ Mg, $m_{ss}=449$ Mg	0.6 m coarse sand Over 3.6 m clay ($s_u=33$ kPa)[a] Over 5.4 m loose sand ($D_r=35\%$) Over dense sand ($D_r=75\%$)	57.2g
DDC02	$b=1.17$ m, $I=24.0\times10^{-3}$ m^4 L, W, $H=14.3$, 9.2, 2.2 m Superstructure $T=0.3$ s[b] $m_{cap}=714$ Mg, $m_{ss}=449$ Mg	0.6 m coarse sand Over 3.6 m clay ($s_u=22$ kPa)[a] Over 5.4 m loose sand ($D_r=35\%$) Over dense sand ($D_r=75\%$)	57.2g

Note: b=pile outer diameter; I=moment of inertia; L=pile cap length; W=pile cap width; H=pile cap thickness; m_{cap}=pile cap mass; m_{ss}=superstructure mass; $E=68.9$ GPa; $\sigma_y=216$ MPa; and N=centrifugal acceleration.

[a]Average s_u value over layer thickness.

[b]Fixed-base natural period.

opposed to a more viscous pore fluid that would be required to simulate the prototype viscosity of water, to avoid any chemical interactions that would occur between a more viscous pore fluid and the clay minerals. Implications of pore fluid viscosity are discussed later. Models were tested in a flexible shear beam container (FSB2) at centrifugal accelerations ranging from 38.1 to 57.2g. Results are presented in prototype units.

The piles were composed of T6-6061 aluminum tubing (E=68.9 GPa) with a thin plastic shrink wrap layer placed around them to protect the electrical resistance strain gauges affixed to the piles. The plastic shrink wrap increases the effective diameter of the piles (diameters were 0.73 and 1.17 m for models spun to 38.1 and 57.2g, respectively), while the flexural stiffness of the pile section was dominated by the aluminum [moment of inertia was 4.5×10^{-3} m^4 (38.1g) and 2.3×10^{-3} m^4 (57.2g)] (Table 1). Fiber analyses of the pile sections with zero imposed axial load, a yield stress of 270 MPa, and an ultimate stress of 310 MPa produce yield moments of 3,320 kN m (38.1g) and 11,240 kN m (57.2g), and ultimate moments of 5,020 kN m (38.1g) and 17,110 kN m (57.2g). The pile response remained within the elastic range for 18 of the 21 test motions, and yielding was limited to the large motions for test SJB01 with a maximum mobilized curvature ductility of 1.2. At this curvature ductility, the inelastic bending moment is only 6% smaller than would be computed using elastic section properties. Hence, bending strain measurements were converted to bending moments using elastic section properties, with acknowledgement that this simplification introduces small errors into the bending moment data for the three large motions for test SJB01. Center-to-center pile spacing was four diameters, and the piles were connected by an embedded pile cap. Good contact between the crust and the pile cap was established by pressing a rectangular cofferdam into the crust, excavating the crust inside the cofferdam, driving the piles into the model at 1g, lowering the pile cap into the excavation, and filling the annulus between the cofferdam and the pile cap with stiff, strong plaster. The pile caps provided a stiff rotational restraint at the pile-to-cap connection with the measured rotational stiffness being about 400 MN·m/rad (38.1g) and 1,300 MN m/rad (57.2g). Single-degree-of-freedom structures with fixed-base natural periods of 0.8 and 0.3 s were connected to the pile cap for tests DDC01 and DDC02, respectively.

Each test was shaken with simulated earthquakes conducted in series with sufficient time between events to allow dissipation of excess pore pressures. The base motions were scaled versions of the acceleration recordings either from Port Island (83 m depth, north–south direction) during the Kobe earthquake, or from the University of California, Santa Cruz (UCSC/Lick Laboratory Channel 1) during the Loma Prieta earthquake. The base motion sequence applied to the models was a small event ($a_{\max,\text{base}}$ =0.13–0.17g) followed by a medium event ($a_{\max,\text{base}}$ =0.30–0.45g) followed by one or more large events ($a_{\max,\text{base}}$ =0.67–1.00g). Complete data reports from the centrifuge tests are available on the Center for Geotechnical Modeling website.

Centrifuge Test Observations

The centrifuge tests helped identify several mechanisms of interaction between piles and liquefied ground that are not included in current guidelines for static analyses. Consider the set of recorded time series shown in Fig. 3 for the pile group in test SJB03 during a large Kobe motion. The plotted bending moment was measured near the pile cap connection in one of the two piles furthest upslope in the group, where the peak bending moments were measured for the tests. The lateral load from the crust is the sum of the loads on the pile cap and on the pile segments within the clay crust. Records of subgrade reaction (p) between the pile and soil and excess pore pressure ratio (r_u) were near the center of the loose sand layer, and r_u was in the free field (about 13 m downslope from the pile group). Displacement of the crust was measured to the side of the pile cap between the cap and the container wall. The data processing procedures used to prepare these time series and more examples of recorded responses are given in Brandenberg et al. (2005).

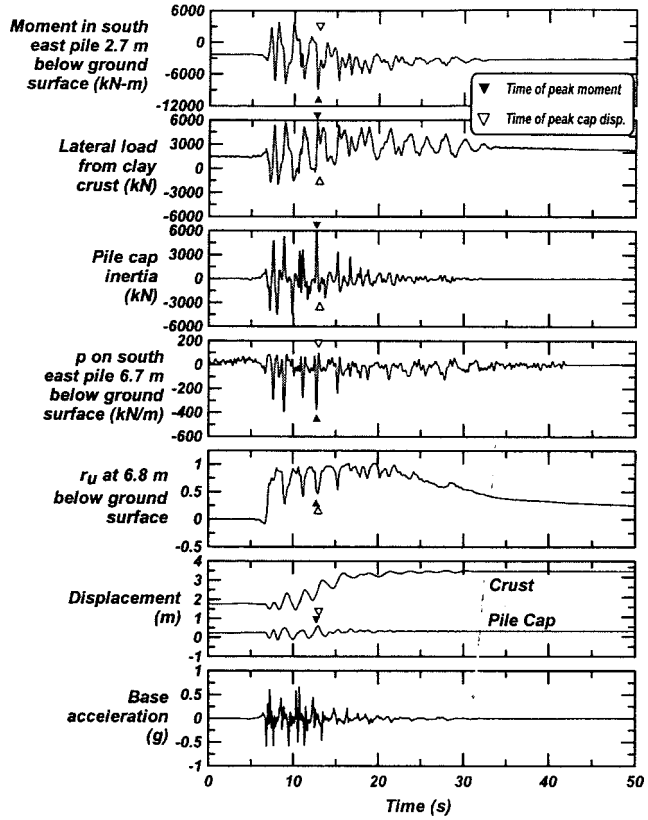

Fig. 3. Time series from test SJB03 for a large Kobe motion (Brandenberg et al. 2005)

At the time that the peak magnitude bending moment (−8,840 kN m) occurred, the lateral load from the clay crust reached a local maximum (5,730 kN), r_u transiently dropped to about 0.5 (it had previously been near 1.0 and subsequently returned to near 1.0), the magnitude of p reached a local maximum (−400 kN/m; the negative sign means the sand restrained downslope movement of the pile), and the pile cap inertia reached a local maximum (6,030 kN). Several additional cycles mobilized bending moments near the measured peak, all of which were associated with transient reductions in pore pressure caused by dilatancy of the sand. Sand that is dense of its critical state (in this case loose sand at low confining stress) tends to dilate at large shear strains under drained loading conditions, and this tendency is manifested as a reduction in pore pressure during undrained loading. Dilatancy significantly affected foundation response in the centrifuge because the loose sand temporarily regained sufficient stiffness and strength to exert large lateral loads on the piles as a reaction against the driving loads exerted by the spreading crust. Furthermore, this transient resistance provided by the liquefiable sand layer contributed to a rapid deceleration of the pile

Table 2. Summary of Estimated Crust Load Components

Test	Passive force (kN)	Side friction (kN)	Base friction (kN)	Force on pile segment in crust (kN)	Predicted crust load (kN)	Measured peak crust load (kN)
PDS03	1,090	490	170	560	2,310	≈2,530[a]
SJB01	2,320	950	350	1,020	4,640	4,980
SJB03	3,500	450	690	2,990	7,630	6,380
DDC01	2,600	650	570	2,160	5,980	6,150
DDC02	2,090	480	410	1,540	4,520	4,330

[a]Pile cap inertia was not measured for test SJB03, so crust load was approximated as peak measured shear force from PDS03 minus cap inertia for the similar Model SJB01.

cap while the crust continued to flow downslope, thereby causing a large inertia load and large crust load to occur simultaneously.

Observations from the suite of centrifuge tests showed that relative displacements between the pile cap and laterally spreading crust required to mobilize peak crust loads ranged from about 1 to 3 m (25 to 70% of the crust thickness), which is an order of magnitude larger than observations from static load tests of pile foundations in nonliquefied ground (e.g., Duncan and Mokwa 2001). Brandenberg (2007) developed simple analytical models that explain how the underlying liquefiable sand softens load transfer behavior by causing horizontal stresses to be distributed throughout a large zone of influence. Other contributors to load transfer softening were cyclic degradation and crack formation within the crust material, which were only approximately incorporated in the analytical models.

Many of the mechanisms that contributed to the pile behavior observed during the centrifuge tests are beyond the scope of static methods. For example, dilatancy significantly affected the foundation response, and can be caused by local strains imposed on the soil by the piles and/or by soil strains induced by ground shaking, which cannot be accurately accounted for using static analyses. Rather than attempting to track every nuance of behavior, static methods seek "statically equivalent" input parameters and loading conditions intended to envelope the peak bending moments and foundation displacements. The reliable application of these BNWF analysis methods requires an evaluation of the resulting bias and dispersion between predicted and observed responses.

Adopted and Recommended Guidelines

This section presents the baseline set of guidelines used to estimate input parameters and loading conditions for the analyses in this paper. Existing guidelines for analyzing piles in nonliquefied ground were adopted and subsequently modified to account for the influence of liquefaction and lateral spreading. Some previous modifications for liquefaction were adopted in this study (e.g., for subgrade reaction in liquefied sand), while the centrifuge test data provided guidance into loading mechanisms that were previously unidentified or characterized with insufficient data (e.g., load transfer between pile caps and spreading crusts). Guidelines presented in this paper are appropriate for pile foundations that are stiff enough to resist the full passive pressures of the laterally spreading crust without exhibiting excessive displacements.

p–y Properties without Influence of Liquefaction

The capacity of $p-y$ elements attached to piles embedded in the nonliquefiable clay crust were computed based on Matlock (1970) static relations for soft clay. Matlock's cyclic $p-y$ relations were not used because they were formulated for sensitive clays under many loading cycles applied at the pile head (e.g., wind or wave loading) that tend to reduce the $p-y$ strength and stiffness, thereby causing pile displacements to increase with repeated cyclic loading. Loading conditions during lateral spreading are significantly different (i.e., a few large soil displacement cycles with a static downslope displacement bias), and lateral spreading soils exert driving forces on the piles rather than resisting forces. Hence, reducing $p-y$ capacity would be incorrect and unconservative for lateral spreading conditions. The empirical factor, J, that appears in Matlock's equations for p_u was taken as 0.5.

Material properties for $p-y$ relations for nonliquefied sand were based on API (1993) guidelines. Typically, a constant coefficient of subgrade reaction (k) is used to derive $p-y$ relations, which inherently assumes that subgrade reaction stiffness increases linearly with depth. However, the elastic modulus of sand approximately increases with the square root of confining stress, and using a constant k value therefore overestimates the stiffness at depths more than a few pile diameters (published k values were derived from static load tests that mobilize primarily the shallow soil layers). This overestimate may not be important for pile head loading, but may contribute significantly when lateral spreading conditions mobilize large loads deep in the soil profile. Hence, the API subgrade reaction moduli were assumed to correspond to a reference vertical stress of 50 kPa and to change in proportion to the square root of vertical effective stress based on the procedure in Boulanger et al. (2003).

The capacity of the $p-y$ elements attached to the pile caps (one $p-y$ element at the top and one at the bottom of the cap) included passive force on the upslope face of the caps and friction forces along the sides and base of the pile caps. Passive earth pressures accounted for wall friction and inertial effects. Side and base friction on the soil–cap interface, (f_u) was estimated as $f_u=\alpha \cdot s_u$, where the relation from Randolph and Murphy (1985) for piles driven into clay was used to estimate $\alpha=0.5$, 0.55, and 0.6 for $s_u/\sigma'_{vc}=1.3$, 0.9, and 0.6 ($s_u=44$, 33, and 22 kPa, and $\sigma'_{vc}=35$ kPa near the base of the pile cap), respectively. Base friction was reduced by 75% (average value estimated for the suite of centrifuge tests) to account for loss of contact between the crust and the base of the pile cap due to settlement and gap formation along the downslope portion of the cap, and interaction between cap base friction and lateral loads on the pile segments in

the clay crust beneath the pile cap. Details on the calculation procedures and results are provided in Brandenberg et al. (2005). The computed crust loads are summarized in Table 2, and were within about 12% of measured peak values with an average overprediction of 2%. The stiffness of the $p-y$ materials in the crust layer (both on the piles and on the pile cap) were set so that the ultimate crust load was mobilized at about 40% of the crust thickness to account for the softening influence of the underlying liquefied sand as estimated by the load transfer models developed by Brandenberg et al. (2007).

t−z Properties without Influence of Liquefaction

Shaft friction was represented using $t-z$ elements distributed along the length of the piles. The capacity of the $t-z$ materials in clay was computed as $t_u=\alpha\cdot s_u\cdot\pi\cdot b$, where the relation from Randolph and Murphy (1985) was used to estimate α. The shape of the $t-z$ curves in clay approximated relations by Reese and O'Neill (1987) for drilled shafts.

The capacity of the $t-z$ materials in sand with free-field $r_u=0$ were computed as $t_u=K\cdot\sigma'_v\cdot\pi\cdot b\tan\delta$, where K was taken as 0.4 as recommended by Reese et al. (2000), and δ was taken as 20 and 30° for loose and dense sand, respectively. The shape of the $t-z$ curves in sand approximated the relations by Mosher (1984). Ultimate capacities of the $t-z$ elements were mobilized at displacements equal to 0.5% of the pile diameter.

Vertical friction forces along the sides of the pile cap were distributed into $t-z$ materials at the back of, and along the length of, the pile cap. The distribution of $t-z$ elements along the length of the cap allows friction forces to counteract rocking of the pile group.

q−z Properties without Influence of Liquefaction

End bearing resistance was represented using $q-z$ elements attached to the pile tips. The capacity of the $q-z$ elements for nonliquefied conditions (i.e., free-field $r_u=0$) were computed based on bearing capacity factors from Meyerhof (1976). The shape of the $q-z$ curves approximated Vijayvergiya (1977) relations for pile in sand, and the ultimate capacity was mobilized at a displacement of 5% of the pile diameter.

Influence of Liquefaction on Soil Springs

The influence of liquefaction (i.e., free-field peak $r_u=1$) on $p-y$ behavior in the sand layers was incorporated by reducing the capacity by factors of 0.05 and 0.3 for loose sand and dense sand, respectively. These reduction factors, called p multipliers (m_p), are consistent with the first-order effects of relative density on undrained shear strength of sand. Fig. 4 shows the relation between m_p and $(N_1)_{60cs}$ recommended by Brandenberg (2005) and by the Architectural Institute of Japan (AIJ 2001). The two recommendations agree reasonably well for loose materials, but Brandenberg recommends lower m_p for dense materials compared with AIJ. For cases in which free-field r_u values were expected to be intermediate between 0 and 1, m_p values were linearly interpolated (e.g., Dobry et al. 1995). There is insufficient data for selection of appropriate multipliers for $t-z$ and $q-z$ materials, so for simplicity, the p multipliers were assumed to characterize the effects of liquefaction on $t-z$ and $q-z$ behavior as well.

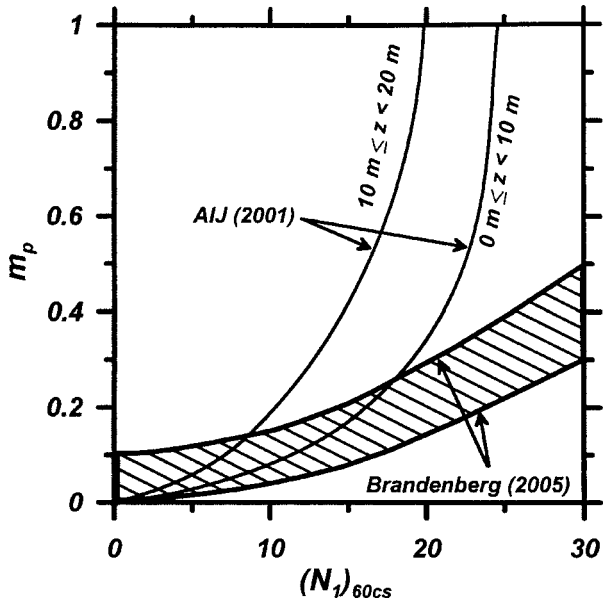

Fig. 4. Summary of recommended p multipliers for liquefied ground

Ground-Displacements

Ground displacements were estimated using a Newmark (1965) sliding block analysis, wherein a residual shear strength ratio for the liquefiable layer ($s_r/\sigma'_{vc}=0.05$) was selected by trial and error until it produced predicted displacements that, on average, matched the observed crust displacements across the suite of centrifuge tests. The sliding block analyses only allowed downslope slip and were performed using the input motion measured at the base of the container. Predicted and observed ground displacements are presented in Table 3. Calibration of residual strength eliminated bias in the prediction of lateral spreading displacements, but did not eliminate dispersion due to the various complexities that are not captured by the Newmark procedure [e.g., oscillations in pore water pressure (see Fig. 3) causing variations in yield acceleration during shaking]. Bias was deliberately removed from the ground displacement prediction because one goal of this study is to evaluate any bias inherent to the monotonic BNWF methods independently from bias in the selected input parameters. It is acknowledged that bias in the input parameters, including ground displacement, would introduce additional bias into predictions of pile response. Cumulative ground displacements (i.e., total predicted displacement for a sequence of motions) were imposed in the BNWF analyses to account for ground displacements from previous motions.

The Newmark sliding block procedure was selected for this study because (1) recorded base motions could be used to estimate sliding displacements; (2) the observed deformation mecha-

Table 3. Ground Surface Displacements for Each Ground Motion

Motion	Predicted ground surface displacement (m)	Measured ground surface displacement (m)
Small Santa Cruz	0.05	0.01–0.04
Medium Santa Cruz	0.15	0.04–0.30
Large Santa Cruz	1.0	0.30–1.60
Large Kobe	1.8	0.80–2.50

nism of the clay sliding on top of the liquefiable sand resembled the mechanism assumed in Newmark methods; and (3) the residual strength of the liquefied sand could be calibrated to match the measured ground displacements. Alternative methods of estimating ground displacement could be more appropriate for design, including the shear strain profile approach (e.g., Ishihara and Yoshimine 1992; Tokimatsu and Asaka 1998), correlations with liquefaction potential index or displacement index (e.g., Kutter et al. 2004; Holzer et al. 2006), empirical correlations (e.g., Bartlett and Youd 1992), or dynamic finite-element analyses. A detailed study of ground displacement prediction methods is beyond the scope of this paper, and use of the Newmark procedure does not constitute preference of this approach for design.

The profile of ground displacement with depth was selected to be consistent with the profile observed during model excavation after the centrifuge tests (see Fig. 1). Small strains were observed in the dense sand layer, and shear strains in the loose sand were largest near the interface between the loose sand and clay. Most of the ground surface displacement was attributed to a displacement discontinuity at the interface between the sand and clay that formed when void redistribution weakened a zone in the loose sand immediately beneath the clay (e.g., Kulasingam et al. 2004). Predicting the discontinuous distribution of soil displacements is quite difficult, so the response of a pile group to a continuous soil displacement profile is explored later.

Structural Inertia Forces

Structural inertia forces were from the embedded pile caps and the structures attached to the pile caps (structures were attached for only two of the five tests in this study: DDC01 and DDC02). Pile cap inertia is often neglected in design based on the assumption that the superstructure is much more massive than the pile cap. However, the pile caps in the centrifuge studies were quite massive (e.g., about 714 Mg compared with a superstructure mass of 449 Mg for tests at 57.2g) because (1) the pile diameters were large; (2) pile cap thickness was about two pile diameters (as required to "fix" the pile head); and (3) center-to-center spacing was four diameters. The large-diameter piles were required to limit pile cap displacements and rotations to reasonable levels under the large lateral loads from the strong nonliquefiable crusts, and the large spacing was required to counteract rocking through axial forces in the piles. Such large piles would not be required to support the superstructure in the absence of lateral spreading, in which case the pile cap mass might be negligible compared with the superstructure. The centrifuge pile foundations demonstrate that inertia forces imposed by pile caps can be important when large diameter piles are used to react against lateral spreading demands.

Selecting inertia forces to use in combination with lateral spreading demands for monotonic BNWF analyses poses two questions: (1) what are the peak anticipated accelerations of the pile cap and superstructure; and (2) what fraction of the peak inertia forces should be combined with lateral spreading demands in static analyses? Design response spectra and site response analyses typically do not account for the influence of liquefaction on ground motion, hence it is useful for design purposes to relate structural accelerations to ground motion that would be anticipated in the absence of liquefaction. Acceleration response spectra for the ground surface motions were estimated from equivalent linear site response analyses using SHAKE91 (Idriss and Sun 1992). Small-strain shear modulus was estimated from measurements of shear wave velocity taken while the centrifuge was spinning before shaking, and modulus reduction and damping curves were based on EPRI (1993) for sand and Vucetic and Dobry (1991) for clay with PI=50. The influence of the model container was incorporated by adding its mass and stiffness contributions into the properties of the soil column.

Table 4. Spectral Accelerations for the Ground Surface Motions Predicted in the Absence of Liquefaction

	Spectral acceleration (g)[a]		
Motion	T=0.0 (s)	T=0.3 (s)	T=0.8 (s)
Small Santa Cruz	0.3	0.4	0.4
Medium Santa Cruz	0.5	0.6	0.6
Large Santa Cruz	0.5	0.8	1.2
Large Kobe	0.6	0.8	1.5

[a]Average values from site response analyses for five models. The spectral values correspond to the peak ground surface acceleration (T=0.0 s) and the fixed-base periods of the superstructures for DDC01 and DDC02.

Pile cap acceleration was estimated as the predicted peak horizontal ground surface acceleration (in the absence of liquefaction), while superstructure acceleration was estimated as the predicted spectral acceleration corresponding to the fixed-base natural period of the superstructure (Table 4). The cap and superstructure accelerations predicted for nonliquefied conditions were about 38 and 56% greater (on average), respectively, than the values observed in the centrifuge tests (with liquefaction). More data are required to quantify how the effects of liquefaction on the structural accelerations should be accounted for in design. Nonetheless, the approach adopted in this paper is believed to be reasonably conservative, pending further studies in this area.

Numerical Methods

The BNWF analyses were performed using the open system for earthquake engineering simulation (OpenSees) developed by researchers at the Pacific Earthquake Engineering Research (PEER) Center. Piles were modeled as beam column elements with elastic section properties. The pile cap was modeled using stiff (effectively rigid) beam column elements connecting the pile heads. Soil springs were modeled as zeroLength elements with PySimple1, TzSimple1, and QzSimple1 materials (Boulanger et al. 2003). The analyses were two-dimensional, and the 2×3 pile group was modeled as a 1×3 pile group with the strength and stiffness of the soil springs and pile elements doubled. Soil displacements were imposed using displacement patterns applied to the free ends of the zero length $p-y$ elements (BNWF_SD), or alternatively limit pressures were applied directly to the nodes on the pile elements (BNWF_LP) in the spreading layers while $p-y$ elements were only used in underlying firm ground. Pile cap inertia forces were modeled using linear load patterns applied to the pile cap nodes, and superstructure inertia forces were represented as a horizontal force and moment (equal to horizontal force times height from the top of the pile cap to the center of mass of the superstructure) applied to the center node of the pile cap.

The analyses were conducted by first applying gravity loading using a constant vertical load pattern, and subsequently imposing the horizontal displacement and inertia load patterns simultaneously. Loads and displacements were imposed incrementally using a static load control integrator, with the size of the increments depending on the nonlinearity in the foundation response.

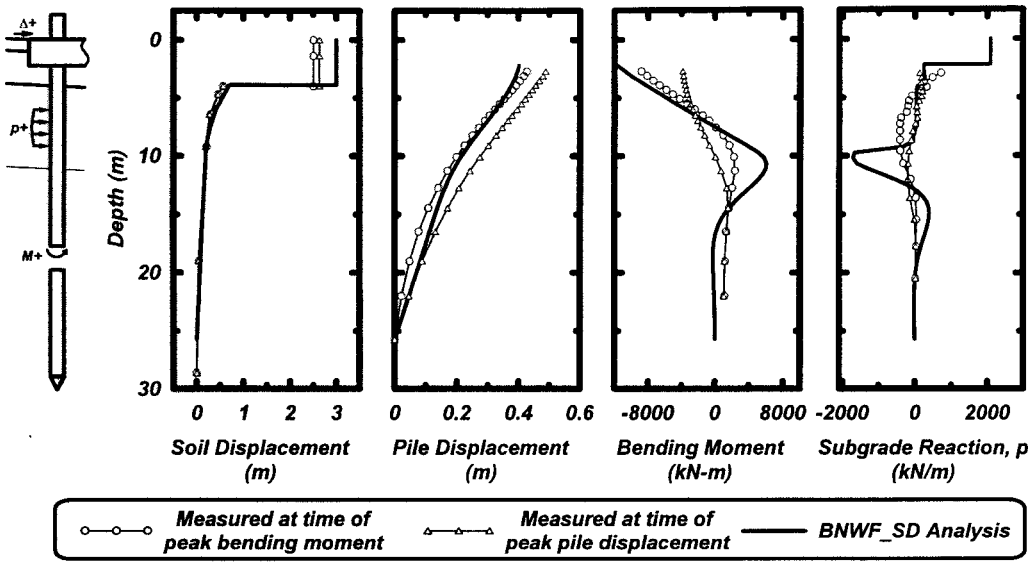

Fig. 5. Results of baseline BNWF_SD analysis of centrifuge test SJB03 for a large Kobe motion

Force convergence was obtained when the norm of the displacement residuals was smaller than a specified tolerance. Penalty constraints were used to enforce the prescribed displacement boundary conditions. Numbering of nodal degrees of freedom was performed using a reverse Cuthill–McKee algorithm, and the system of equations was set up and solved using a Newton–Raphson algorithm.

Baseline Analyses

This section compares bending moments and pile displacements measured during the centrifuge tests with those predicted by static BNWF analyses that utilized the baseline set of input parameters. Distributions of bending moment, pile displacement, and subgrade reaction are presented first for one event, followed by comparisons between the peak bending moments and pile cap displacements for the suite of centrifuge test data. The peak measured bending moments in the piles were from Wheatstone full bridge strain gauge recordings nearest to, but slightly below, the bottom of the pile cap. Predicted peak bending moments occurred at the connection between the piles and pile cap, but comparisons are made at the depth of the Wheatstone bridge for consistency with measured data.

SJB03 Large Kobe Motion

Comparison between the predicted and measured profiles of displacements, bending moments, and subgrade reaction loads (p) are shown in Fig. 5 for a BNWF_SD analysis of the large Kobe motion for test SJB03. Measured peak bending moments and measured peak pile cap displacements occurred at different times during shaking, and snapshots of the distributions are presented at both times. The predicted peak bending moment magnitude (−10,830 kN m) was 23% larger than the measured value (−8,840 kN m), and the predicted peak pile cap displacement (0.40 m) was 17% smaller than the measured value (0.48 m).

Bending moments were predicted reasonably well near the ground surface where the peaks occurred, but not as well deeper in the soil profile. For example, the predicted maximum positive bending moment at about 10 meters depth was considerably larger than the corresponding measured value (+6,040 kN m compared to +2,350 kN m in Fig. 5). The cause of this behavior was the analytical assumption that the capacities of the $p-y$ materials on the piles in the liquefiable sand were very small, in contrast to the significant upslope resisting forces mobilized against the pile by the loose sand layer during the centrifuge tests (see Figs. 3 and 5).

Suite of Centrifuge Tests

Analyses were performed for a suite of five centrifuge tests consisting of 21 different shaking events total, and results of predicted versus measured bending moments and cap displacements are presented in Fig. 6 for the baseline set of input parameters. Bending moments were overpredicted on average by 23%, and pile cap displacements were underpredicted on average by 21% (Table 5). The standard deviation in natural log units of measured versus predicted values was 0.29 for bending moments and 0.25 for pile cap displacements. Statistical analyses of the small data set of 21 cases are presented as qualitative measures of bias and dispersion for comparison among the various assumptions in the BNWF analyses. Statistical analysis of small data sets can cause underprediction of dispersion (e.g., Christian 2004).

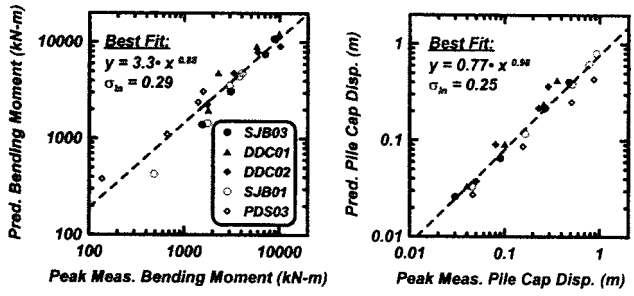

Fig. 6. Baseline BNWF_SD analyses with imposed free-field soil displacements

Table 5. Summary of BNWF Analysis Results

Analysis variation	Bending moment				Pile cap displacement			
	% Error[a]	a[b]	b[b]	σ_{ln}[c]	% Error[a]	a[b]	b[b]	σ_{ln}[c]
Baseline	−8 to +69	3.3	0.88	0.29	−38 to −6	0.77	0.98	0.25
Measured structural inertia forces, ultimate crust load, and ground displacements	−4 to +64	3.4	0.86	0.21	−47 to +1	0.63	0.92	0.31
Limit pressures instead of soil displacements	+12 to +295	746.5	0.26	0.25	−38 to +365	0.46	0.32	0.55
Neglect inertia forces	−53 to +14	2.9	0.83	0.44	−58 to −31	0.71	1.16	0.27
Neglect friction between crust and cap	−13 to +45	2.9	0.89	0.29	−43 to −11	0.68	0.96	0.28

[a]% Error=(predicted-measured)/measured×100% (16th and 84th percentile values are reported).

[b]Form of best fit curve is predicted=a×measured b (see Figs. 6, 7, and 9–11).

[c]σ_{ln}=SD[ln(predicted)−ln(a×measured b)].

Pile cap displacements were accurately predicted for the 1.17 m diameter piles (3% underprediction on average) and underpredicted for the 0.73 m diameter piles (31% underprediction on average). Pile cap rotations that accumulated during the sequence of base motions indicated that axial failure occurred at the tips of the 0.73 m diameter piles (about 0.03 rad residual cap rotation), while cap rotations did not accumulate for the 1.17 m diameter piles (0.00 rad residual cap rotation). Brandenberg et al. (2006) explained that axial failure of piles during lateral loading can cause pile groups to exhibit cyclic ratcheting, wherein pile cap displacements accumulate during repeated loading cycles due to rigid body rotations of the pile groups. The influence of cyclic ratcheting is not captured in the monotonic soil displacement paths used in the BNWF analyses in this paper, which helps explain the underprediction of cap displacements for the 0.73 m diameter pile groups. Failure to adequately model the rigid body pile displacement mechanism also explains how pile cap displacements could be underpredicted while bending moments were overpredicted.

Alternative Guidelines

This section focuses on the influence of alternative design guidelines or approximations (i.e., different from those in the baseline case) on predicted bending moments and pile cap displacements. First, the analyses are repeated using measured values for inertia forces, crust loads, and soil displacements as inputs. Then, the baseline analyses are repeated but with alternative guidelines that include: (1) imposing limit pressures instead of soil displacements; (2) neglecting inertia forces; (3) neglecting friction forces between pile caps and spreading crusts; and (4) using an alternative soil displacement profile shape. Each analysis in this section utilized the baseline set of input parameters with the exception of the noted alternative approximation.

Measured Parameters Used as Inputs

Inertia forces, ultimate crust loads, and ground displacements measured during the centrifuge tests were used in the BNWF analyses in place of the baseline values (Fig. 7) to identify bias and dispersion caused by inaccuracies in input parameters and loading conditions compared with bias and dispersion caused by fundamental limitations of the static BNWF approach. Using these measured input parameters improved bending moment predictions (8 versus 23% overprediction on average) but worsened cap displacement predictions (32 versus 21% overprediction on average). At the same time, the dispersion was reduced for both bending moment and pile cap displacements. The bias in predictions of cap displacements, despite having used these measured input parameters, indicates that static BNWF analyses are not adequately approximating some key phenomena for at least some of the tests, which may include the accumulation of permanent pile cap rotations and displacements due to cyclic ratcheting over the course of the successive shaking events. These limitations, and their contributions to systematic bias in predictions, need to be recognized and accounted for in design.

Limit Pressures Instead of Soil Displacements

BNWF_LP analyses were performed by removing the soil springs in the crust layer and liquefiable sand layer, and replacing them with limit pressures equal to the capacities of the $p-y$ materials. Analysis results are presented in Fig. 8 for a large shaking motion event for test SJB03. The predicted peak bending moment (−9,544 kN m) was 8% larger than the measured value (−8,840 kN m), and the predicted pile cap displacement (0.20 m) was 58% smaller than the measured value (0.48 m). Comparing the BNWF_LP and BNWF_SD analysis results for this case (Figs. 5 and 8), the BNWF_LP analysis gave similar bending moments but considerably smaller cap displacements. In the BNWF_LP analysis, strains were not applied in the dense sand layer because the primary reason for utilizing limit pressures in-

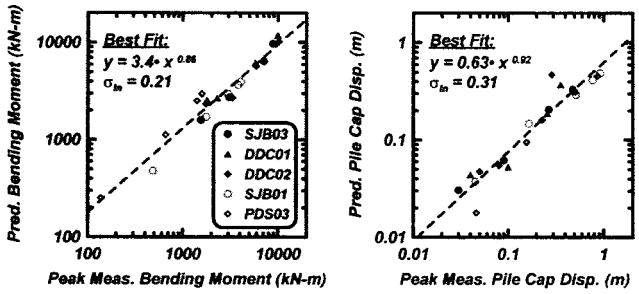

Fig. 7. Baseline BNWF_SD analyses, but with measured inertia forces, ultimate crust loads, and soil displacements as inputs

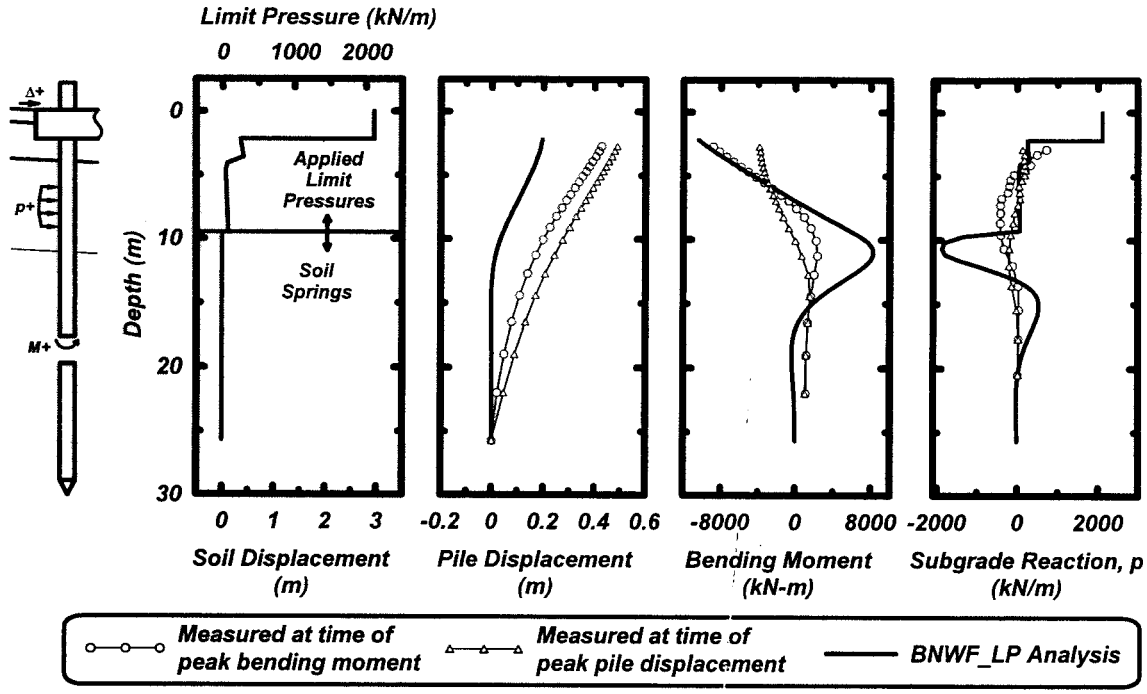

Fig. 8. Results of BNWF_LP analysis of centrifuge test SJB03 for a large Kobe motion

stead of soil displacements is to avoid the sometimes difficult task of imposing displacement boundary conditions. Soil displacements in deep layers can significantly affect displacements at the pile head, and this is why the BNWF_LP gave poor (unconservative) results for the pile cap displacement in this case.

Predicted versus measured bending moments and cap displacements for the suite of shaking events are shown in Fig. 9 for analyses with imposed limit pressures. Bending moments and pile cap displacements were greatly overpredicted for the small motions because the limit pressures approach inherently assumes ground displacements are large enough to mobilize the ultimate capacities of the $p-y$ materials, which was true of the large motions but not of the small and medium motions. For the larger motions, the bending moments are more reasonably predicted, while the pile cap displacements now tend to be underpredicted for the reason described previously (i.e., Fig. 8).

Neglecting Structural Inertia Forces

Structural inertia forces are often not imposed simultaneously with crust loads based on the assumption that the two load components occur at different times (e.g., TRB 2002). Baseline BNWF_SD analyses were repeated without imposing any pile cap or superstructure inertia forces to observe the influence of this assumption on the analysis results (Fig. 10). Bending moments were underpredicted by an average of 38% and pile cap displacements were underpredicted by an average of 42%. These BNWF analyses underpredicted bending moments and cap displacements because peak inertia forces occurred nearly simultaneously with peak crust loads in some centrifuge models. Inertia forces contributed significantly to lateral loading, and neglecting them in design for conditions similar to those in the centrifuge tests would be unconservative. Selecting appropriate inertia forces to use in combination with lateral spreading demands is not clearly understood at this time, but including a first-order estimate of inertia forces is certainly better than neglecting them.

Neglecting Friction Forces on Pile Caps

Friction forces between the spreading crust and the sides and base of the pile cap are typically not explicitly required in design guidelines (e.g., JRA 2002), and are therefore often neglected

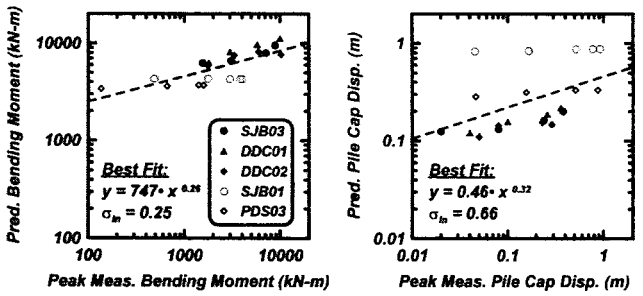

Fig. 9. Baseline analyses, but with imposed limit pressures (BNWF_LP) instead of ground displacements (BNWF_SD)

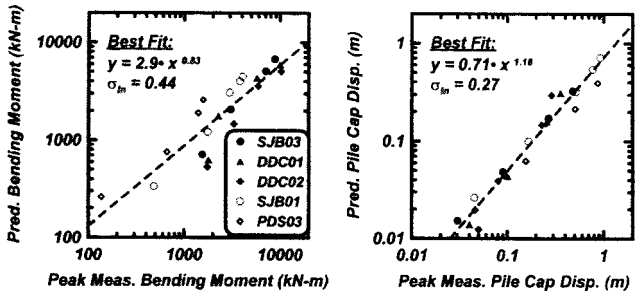

Fig. 10. Baseline BNWF_SD analyses, but neglecting pile cap and superstructure inertia loading

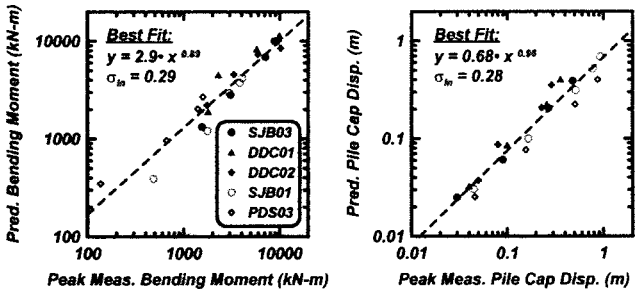

Fig. 11. Baseline BNWF_SD analyses, but neglecting friction forces on pile cap

based on the assumption that passive forces dominate the ultimate lateral loads. Fig. 11 shows predicted versus measured values of bending moment and pile cap displacement for BNWF analyses with the friction component excluded from the ultimate crust load on the pile cap. Bending moments are underpredicted by an average of 13% and pile cap displacements are underpredicted by an average of 29%. Friction forces were not a dominant factor, but were also not a negligible factor with regard to the pile foundation response, and should be included in crust load estimates. The influence of friction on total lateral crust load depends on soil properties and pile cap geometry, and could be smaller or larger than the influence observed in this study.

Alternative Ground-Displacement Profile Shape

The centrifuge test data exhibited a displacement discontinuity at the interface between the crust and the underlying loose sand, and this displacement profile was incorporated into the analyses in this paper. However, displacement discontinuities are difficult to predict, so assessing the sensitivity of the analytical predictions to various displacement profile shapes may be insightful. For example, the BNWF_SD analysis for a large Kobe motion for test SJB03 (see Fig. 5) was repeated with the only change being a continuous soil profile in which the strains in the loose sand layer were increased to accommodate the crust displacement (Fig. 12). Predicted peak bending moment magnitude increased by only 3% while predicted cap displacement increased by only 5% compared with the baseline case. The predictions are relatively insensitive to the ground displacement profile in this analysis because the capacities of the $p-y$ springs in the liquefied layer were small and the pile group response was dominated by crust loads and inertia loads.

More flexible pile foundations would be expected to be more significantly influenced by the ground displacement profile, and observing the sensitivity of the predicted pile response to ground displacement profile is recommended.

Discussion

Crust loads and structural inertia loads measured in the centrifuge tests acted nearly in phase during critical cycles for the large motions for the 1.17 m diameter pile groups (95–100% of the peak structural inertia force acted simultaneously with the peak crust load), but not for the 0.73 m diameter pile groups (25–37% of the peak structural inertia force acted simultaneously with the peak crust load). Peak downslope inertia forces occurred when the pile cap decelerated and came to a halt, hence inertia forces and lateral spreading forces acted in phase when the pile group was stiff enough to cause the pile cap and superstructure to quickly decelerate even as the crust exerted its ultimate pressure on the foundation. Structural inertia forces did not act in phase with crust loads for more flexible pile foundations that accumulated large permanent rotations and displacements during the lateral spreading. Potential damage to the structure caused by large foundation displacements typically renders flexible foundations unacceptable, so design guidelines in this paper focus on stiff pile foundations and may overestimate loads for more flexible foundations. Additional research is required to clarify the appropriate selection of inertia loads to impose simultaneously with lateral spreading demands for a range of different foundation properties and soil properties.

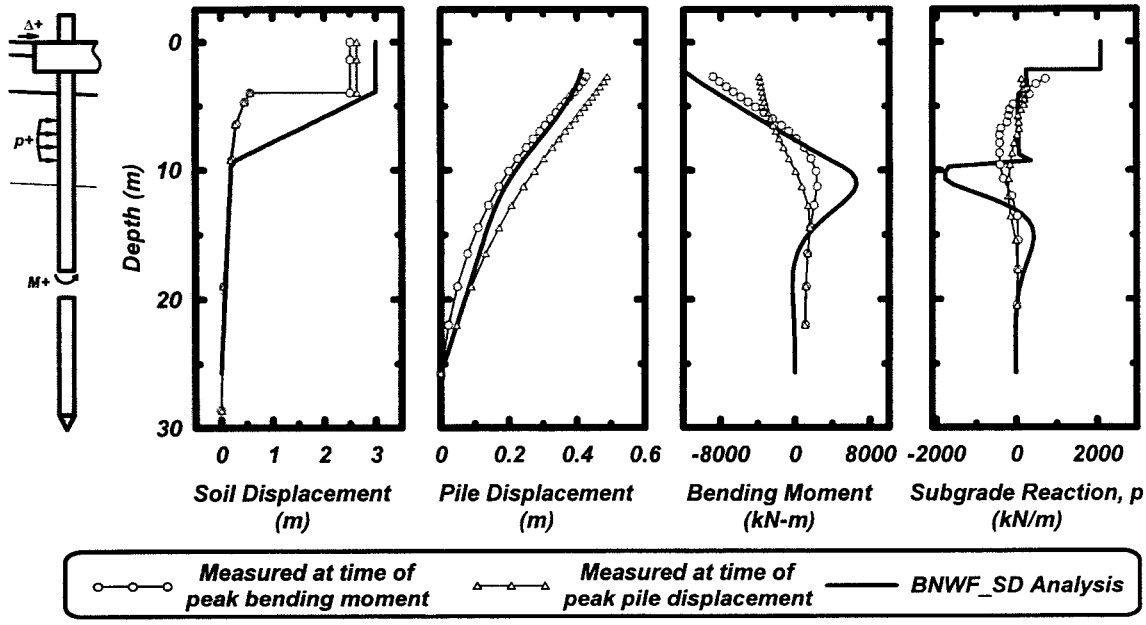

Fig. 12. BNWF_SD analysis of centrifuge test SJB03 for a large Kobe motion with a continuous free-field ground-displacement profile

Some of the baseline input parameters were calibrated to fit, on average, the suite of centrifuge test data so that bias introduced by parameter selection could be separated from bias associated with the BNWF method itself. Bias from predicted ground displacements was reduced by calibrating the selection of the liquefied sand's residual strength for the Newmark sliding block procedure to fit the suite of centrifuge test data. Methods for estimating ultimate crust loads were calibrated to match, on average, the centrifuge test data. Uncertainty in the ground motion was not considered in the present study because the base motions were known. Including these and other additional sources of uncertainty would be expected to significantly increase the dispersion between predicted and measured bending moments and cap displacements.

This paper focused on analysis of isolated pile groups and simple superstructures, while lateral spreading demands affect entire bridges and not just isolated foundations. Extending the guidelines presented in this study to entire bridge systems will require considerable judgment pending additional studies of complete bridge systems.

Water was used as a pore fluid in the centrifuge models, hence the prototype permeability is N-times that of the model based on the adopted scaling factors (N=centrifugal acceleration). This means that the prototype permeability is more representative of a coarse sand than the fine sand used in the models. Permeability affects the rate of excess pore water pressure diffusion around the piles and thereby affects the subgrade reaction behavior, as discussed in Wilson et al. (2000) and more recently demonstrated in centrifuge experiments by Gonzales (2005) and numerical simulations by Uzuoka et al. (2005). The effects of excess pore water pressure diffusion, both during and after shaking, on the ground displacement profile and soil-pile subgrade reaction behavior are difficult to incorporate into simplified design methodologies. For this reason, uncertainties in the soil permeability and its effects on system response (whether in a centrifuge or the field) are an additional source of potential bias and dispersion in BNWF analyses.

The peak bending moment in the piles in the experiments was at the fixed connection with the pile cap and this peak was reasonably predicted by the recommended method. Bending moments deeper in the soil profile were not predicted well, but these errors were not considered critical because the pile design would likely be controlled by bending moments at the pile cap connection. The errors deeper in the profile were caused by errors in modeling subgrade reaction in the loose sand layer. Large upslope resisting loads were measured at the time of the peak bending moment, but the capacity of the $p-y$ springs in the analytical models was much smaller. To improve the prediction of bending moments deeper in the ground it would be necessary to (1) use a more sophisticated model for the $p-y$ behavior in the loose sand that captures the influence of dilatancy; and (2) have an accurate knowledge of the transient and permanent displacement profile in the ground.

Summary and Conclusions

Static beam on nonlinear Winkler foundation analyses and design guidelines were evaluated against a suite of centrifuge test data of pile foundations in liquefied and laterally spreading ground. The pile foundations were six-pile groups of either 0.73 or 1.17 m diameter piles connected together by a pile cap that was embedded in a mildly sloping profile consisting of a clay crust overlying loose sand overlying dense sand. Design guidelines were proposed that account for recent findings regarding soil-pile interaction mechanisms during liquefaction-induced lateral spreading. The proposed guidelines were developed for pile foundations that are sufficiently stiff and strong to limit their lateral displacements while the surrounding ground spreads past it. Lateral spreading demands were represented either by imposing free-field soil displacements to the free ends of the $p-y$ elements (BNWF_SD) or by imposing limit pressures directly to the pile nodes (BNWF_LP). A single baseline set of input parameters was used to analyze a total of 21 cases using the BNWF_SD approach, after which alternative design guidelines and approaches were similarly evaluated.

The BNWF_SD analyses using the proposed guidelines and a single set of baseline parameters provided reasonable predictions for the suite of centrifuge test data, with the pile bending moments overpredicted on average (16th and 84th percentile errors were -8 and $+69\%$, respectively) and pile cap displacements underpredicted on average (16th and 84th percentile errors were -38 and -6%, respectively). The BNWF_SD analyses were more accurate for the stiffer 1.17 m diameter pile groups than for the more flexible 0.73 m diameter pile groups because (1) pushover methods do not capture cyclic ratcheting (i.e., the accumulation of permanent displacement and rotation during repeated loading cycles, as occurred for the 0.73 m diameter pile groups) and (2) the assumption of lateral spreading forces acting simultaneously with structural inertia forces is most reasonable for the stiffer pile foundations, but slightly conservative for the more flexible pile groups. BNWF_SD analyses that neglected structural inertia forces significantly underpredicted bending moments (16th and 84th percentile errors were -53 and $+14\%$, respectively) and cap displacements (16th and 84th percentile errors were -58 and -31%, respectively). The alternative BNWF_LP analyses: (1) provided reasonable predictions of bending moments for the large motions, but overpredicted bending moments for small and medium motions because ground displacements during these motions were too small to mobilize the presumed limit pressures, and (2) underpredicted pile cap displacements for the large motions because shear strains that occurred in the underlying nonliquefied layer were not included in the analyses, but overpredicted pile cap displacements for the small and medium motions because the ground displacements were too small to mobilize the presumed limit pressures.

The static BNWF pushover analysis method has fundamental limitations that contribute to both dispersion and potential bias in predictions of pile bending moments and pile cap displacements, yet the method may be acceptable for design if this bias and dispersion is recognized and appropriately accommodated. The potential benefits of more sophisticated analytical approaches can then be evaluated in terms of the anticipated reductions in bias and dispersion that they may provide.

Acknowledgments

Funding was provided by Caltrans under Contract Nos. 59A0162 and 59A0392 and by the Pacific Earthquake Engineering Research Center, through the Earthquake Engineering Research Centers Program of the National Science Foundation, under Contract No. 2312001. The contents of this paper do not necessarily represent a policy of either agency or endorsement by the state or federal government. The centrifuge shaker was designed and constructed with support from the National Science Foundation

(NSF), Obayashi Corp., Caltrans, and the University of California. Recent upgrades have been funded by NSF Award No. CMS-0086588 through the George E. Brown, Jr., Network for Earthquake Engineering Simulation. Center for Geotechnical Modeling (CGM) facility manager, Dan Wilson, and CGM staff T. Kohnke, T. Coker, and C. Justice provided assistance with centrifuge modeling; P. Singh collected and processed some of the centrifuge test data. Dr. I. M. Idriss provided helpful insights for the first writer's Ph.D. dissertation, many of which are reflected in this paper. The writers appreciate all of the above support and assistance.

References

American Petroleum Institute (API). (1993). *Recommended practice for planning, design, and constructing fixed offshore platforms, API RP 2A–WSD*, 20th Ed., API, Washington, D.C.

Architectural Institute of Japan (AIJ). (2001). *Recommendations for design of building foundations*, AIJ, Tokyo (in Japanese).

Bartlett, S. F., and Youd, T. L. (1992). "Empirical analysis of horizontal ground displacement generated by liquefaction-induced lateral spread." *Technical Rep. NCEER-92-0021*, National Center for Earthquake Engineering Research, Buffalo, N.Y.

Boulanger, R. W., Kutter, B. L., Brandenberg, S. J., Singh, P., and Chang, D. (2003). "Pile foundations in liquefied and laterally spreading ground during earthquakes: Centrifuge experiments and analyses." *Rep. UCD/CGM-03/01*, Center for Geotechnical Modeling, Univ. of California at Davis, Davis, Calif.

Boulanger, R. W., and Tokimatsu, K. (2006). "Seismic performance and simulation of pile foundations in liquefied and laterally spreading ground." *Geotechnical Special Publication No. 145*, ASCE, Reston, Va.

Brandenberg, S. J. (2005). "Behavior of pile foundations in liquefied and laterally spreading ground." Ph.D. dissertation, Univ. of California at Davis, Davis, Calif.

Brandenberg, S. J., Boulanger, R. W., Kutter, B. L., and Chang, D. (2005). "Behavior of pile foundations in laterally spreading ground during centrifuge tests." *J. Geotech. Geoenviron. Eng.*, 131(11), 1378–1391.

Brandenberg, S. J., Boulanger, R. W., Kutter, B. L., and Chang, D. (2006). "Monotonic and cyclic beam on nonlinear Winkler foundation analyses of pile foundations in laterally spreading ground." *Proc., 8th U.S. Conf. on Earthquake Engineering*, Paper No. 8NCEE-001480, San Francisco.

Brandenberg, S. J., Boulanger, R. W., Kutter, B. L., and Chang, D. (2007). "Liquefaction-induced softening of load transfer between pile groups and laterally spreading crusts." *J. Geotech. Geoenviron. Eng.*, 133(1), 91–103.

Christian, J. T. (2004). "Geotechnical engineering reliability: How well do we know what we are doing?" *J. Geotech. Geoenviron. Eng.*, 130(10), 985–1003.

Dobry, R., Taboada, V., and Liu, L. (1995). "Centrifuge modeling of liquefaction effects during earthquakes." *Proc., 1st Int. Conf. on Earthquake Geotechnical Engineering*, K. Ishihara, ed., Vol. 3, Balkema/Rotterdam/The Netherlands, Tokyo, 1291–1324.

Duncan, M. J., and Mokwa, R. L. (2001). "Passive earth pressures: Theories and tests." *J. Geotech. Geoenviron. Eng.*, 127(3), 248–257.

Electric Power Research Institute (EPRI). (1993). *Guidelines for determining design basis ground motions*, Vol. 1, Electric Power Research Institute, Palo Alto, Calif.

Gonzales, L. (2005). "Centrifuge modeling of permeability and pinning reinforcement effects on pile response to lateral spreading." Ph.D. dissertation. Rensselaer Polytechnic Institute, Troy, N.Y.

Holzer, T. L., Blair, L. J., Noce, T. E., and Bennett, M. J. (2006). "Predicted liquefaction of east bay fills during a repeat of the 1906 San Francisco earthquake." *Earthquake Spectra*, 22(S2), S261–S278.

Idriss, I. M., and Sun, J. I. (1992). "SHAKE91: A computer program for conducting equivalent linear seismic response analyses of horizontally layered soil deposits." *User's guide*, Univ. of California at Davis, Davis, Calif.

Ishihara, K., and Yoshimine, M. (1992). "Evaluation of settlements in sand deposits following liquefaction during earthquakes." *Soils Found.*, 32(1), 173–188.

Japan Road Association (JRA). (2002). *Specifications for highway bridges*, Public Works Research Institute and Civil Engineering Research Laboratory, Tokyo.

Japanese Geotechnical Society (JGS). (1996). *Special issue on geotechnical aspects of the January 17, 1995, Hyogoken-Nambu Earthquake*, Soils and Foundations, Tokyo.

Japanese Geotechnical Society (JGS). (1998). *Special issue No. 2 on geotechnical aspects of the January 17, 1995, Hyogoken-Nambu Earthquake*, Soils and Foundations, Tokyo.

Kulasingam, R., Malvick, E. J., Boulanger, R. W., and Kutter, B. L. (2004). "Strength loss and localization at silt interlayers in slopes of liquefied sand." *J. Geotech. Geoenviron. Eng.*, 130(11), 1192–1202.

Kutter, B. L., Gajan, S., Manda, K. K., and Balakrishnan, A. (2004). "Effects of layer thickness and density on settlement and lateral spreading." *J. Geotech. Geoenviron. Eng.*, 130(6), 603–614.

Matlock, H. (1970). "Correlations of design of laterally loaded piles in soft clay." *Proc., Offshore Technology Conf.*, Houston, Vol. 1, 577–594.

Meyerhof, G. G. (1976). "Bearing capacity and settlement of pile foundations." *J. Geotech. Engrg. Div.*, 102(3), 195–228.

Mosher, R. L. (1984). "Load transfer criteria for numerical analysis of axial loaded piles in sand." U.S. Army Engineering and Waterways Experimental Station, Automatic Data Processing Center, Vicksburg, Miss.

Newmark, N. M. (1965). "Effects of earthquakes on dams and embankments." *Geotechnique*, 15(2), 139–160.

Randolph, M. F., and Murphy, B. S. (1985). "Shaft capacity of driven piles in clay." *Proc., 1985 Offshore Technology Conf*, Paper OTC4883, 371–378.

Reese, L. C., and O'Neill, M. W. (1987). "Drilled shafts: Construction procedures and design methods." *Rep. No. FHWA-HI-88-042*, U.S. Dept. of Transportation, Federal Highway Administration, Office of Implementation, McLean, Va.

Reese, L. C., Wang, S. T., Isenhower, W. M., Arrelaga, J. A., and Hendrix, J. A. (2000). *LPILE plus version 4.0m*, Ensoft, Inc., Austin, Tex.

Tokimatsu, K., and Asaka, Y. (1998). "Effects of liquefaction-induced ground displacements on pile performance in the 1995 Hyogoken-Nambu earthquake." *Soils Found.*, 163–177.

Transportation Research Board (TRB). (2002). "Comprehensive specification for the seismic design of bridges." *National Cooperative Highway Research Program Rep. 472*, National Research Council, Washington, D.C.

Uzuoka, R., Sento, N., and Kazama, M. (2005). "Numerical analysis of rate-dependent reaction of pile in saturated or liquefied soil." *Proc., Seismic Performance and Simulation of Pile Foundations in Liquefied and Laterally Spreading Ground*, *Geotechnical Special Publication No. 145*, ASCE, Reston, Va., 204–217.

Vijayvergiya, V. N. (1977). "Load-movement characteristics of piles." *Proc., Ports 77 Conf.*, ASCE, New York.

Vucetic, M., and Dobry, R. (1991). "Effect of soil plasticity on cyclic response." *J. Geotech. Engrg.*, 117(1), 89–107.

Wilson, D. W., Boulanger, R. W., and Kutter, B. L. (2000). "Observed seismic lateral resistance of liquefying sand." *J. Geotech. Geoenviron. Eng.*, 126(10), 898–906.